Journal of Hunan University (Natural Sciences)

Vol. 53 No. 6

June 2026

Available online at

https://jonuns.com

Open Access Article

https://doi.org/10.55463/issn.1674-2974.53.6.13

Response Surface Optimization and LC–MS Fingerprinting of Low-Citrinin Yellow Pigments from *Monascus purpureus*

Lina Rahmawati Rizkuloh [1], Slamet Ibrahim [2], Marlia Singgih [1]*

[1] Department of Pharmacochemistry, School of Pharmacy, Institut Teknologi Bandung, Bandung 40132, Indonesia,

[2] Faculty of Pharmacy, Universitas Jenderal Achmad Yani, Cimahi 40633, Indonesia,

* Corresponding author: marlia@itb.ac.id

Article History:

Received: May 5, 2026
Revised: June 13, 2026
Accepted: June 18, 2026
Published: June 30, 2026

Abstract: *Monascus purpureus* is a promising microbial source of natural yellow pigments; however, citrinin contamination limits its application in food, pharmaceutical, and cosmetic products. This study aimed to optimize the production of low-citrinin yellow pigments from M. purpureus using rice-based solid-state fermentation and to characterize the optimized extract through LC–MS/PDA fingerprinting. A modified Central Composite Design under Response Surface Methodology was applied to evaluate the effects of $NaNO_3$, methionine, glycerol, fermentation temperature, and cultivation time on yellow pigment production and citrinin concentration. The optimal conditions were achieved without $NaNO_3$ supplementation, with 0.24% methionine and 2% glycerol, at a fermentation temperature of 28°C and a cultivation time of 16 days. Under these conditions, yellow pigment production reached 2,438.88 ± 46.04 OD units/g, while citrinin concentration decreased to 0.1801 ± 0.0082 mg/kg. Compared with the basal medium, these results represented a 2.22-fold increase in yellow pigment production and a 52.91-fold reduction in citrinin concentration. LC–MS/PDA fingerprinting revealed multiple UV–Vis-active chromatographic features, supporting the chemical traceability of the optimized fermented extract without claiming definitive compound identification. These findings demonstrate that multi-response optimization of fermentation

conditions can improve both the productivity and safety profile of M. purpureus-derived yellow pigments for further development as natural colorants.

Keywords: *Monascus purpureus*; Yellow pigment; Citrinin mitigation; Response surface methodology; Solid-state fermentation; LC–MS/PDA fingerprinting; Natural colorant.

基于响应面法优化与 LC–MS 指纹图谱分析的 Monascus purpureus 低桔霉素黄色素研究

摘要：Monascus purpureus 是一种具有应用潜力的天然黄色素微生物来源；然而，桔霉素污染限制了其在食品、药品和化妆品中的应用。本研究旨在利用以大米为基质的固态发酵优化 M. purpureus 低桔霉素黄色素的生产，并通过 LC-MS/PDA 指纹图谱分析对优化后的提取物进行表征。本研究采用响应面法下的改良中心复合设计，评估 $NaNO_3$、蛋氨酸、甘油、发酵温度和培养时间对黄色素产量及桔霉素浓度的影响。最佳条件为不添加 $NaNO_3$，添加 0.24% 蛋氨酸和 2% 甘油，发酵温度为 28° C，培养时间为 16 天。在该条件下，黄色素产量达到 2,438.88 ± 46.04 OD units/g，而桔霉素浓度降低至 0.1801 ± 0.0082 mg/kg。与基础培养基相比，黄色素产量提高了 2.22 倍，桔霉素浓度降低了 52.91 倍。LC-MS/PDA 指纹图谱分析显示出多个具有 UV-Vis 活性的色谱特征峰，支持了优化发酵提取物的化学可追溯性，但并不意味着对化合物进行了确定性鉴定。研究结果表明，发酵条件的多响应优化能够提高 M. purpureus 来源黄色素的产量和安全性，为其作为天然着色剂的进一步开发提供了依据。

关键词：Monascus purpureus；黄色素；桔霉素控制；响应面法；固态发酵；LC–MS/PDA 指纹图谱；天然着色剂。

1. Introduction

Natural pigments produced by filamentous fungi have received increasing attention as bio-based ingredients for food, pharmaceutical, and cosmetic applications, particularly in response to growing concerns regarding synthetic colorants and chemically derived additives [1]. Among pigment-producing fungi, *Monascus purpureus* has been extensively recognized as a valuable microbial platform because it produces structurally diverse azaphilone pigments, including yellow pigments such as monascin and ankaflavin, as well as orange and red derivatives. These pigments are not only relevant as natural colorants but also as functional metabolites with reported antibacterial, anti-inflammatory, anticancer, hepatoprotective, and metabolic-regulating properties [2–4]. In food systems, *Monascus*-derived pigments have been applied as additives, natural colorants, and potential substitutes for nitrite in meat products, whereas in pharmaceutical and cosmetic contexts their biological activities provide additional value beyond coloration [2]. Thus, *M. purpureus* fermentation represents an important intersection between microbial biotechnology, functional food development, and natural product-based ingredient innovation.

The relevance of *Monascus* fermentation is further supported by earlier work on angkak or red mold rice, a traditional fermented rice product produced using *Monascus* mold. Angkak has historically been associated with food coloration and antioxidant potential, while rice-based fermentation provides a nutritionally suitable solid substrate for fungal growth and secondary metabolite production [5]. Previous studies reported that *M. purpureus* grown on rice can

generate yellow, orange, and red pigments, with the major pigments including monascorubrin and monascoflavin, and with angkak also reported to contain lovastatin [6]. Rice substrate characteristics may also influence biological activity. White rice generally contains approximately 20% amylose, whereas red and black rice contain anthocyanin-related pigments and flavonoid compounds that can contribute to antioxidant activity. In a comparative study, antioxidant activity increased in white rice after fermentation from 18.40% to 21.24%, whereas red rice decreased from 39.50% to 22.20% and black rice slightly decreased from 46.20% to 45.01%, indicating that substrate pigmentation can alter the contribution of fungal and rice-derived metabolites to the final fermented product [7,8].

Despite this promising industrial and biological potential, the broader utilization of *M. purpureus* pigments remains constrained by the possible formation of citrinin, a polyketide mycotoxin that may occur during *Monascus* fermentation [9]. This safety issue is particularly critical when the fermented product is intended for use in food, nutraceutical, pharmaceutical, or cosmetic applications. The challenge is not merely to enhance pigment yield but to control the metabolic balance between desirable pigment biosynthesis and undesirable citrinin accumulation. Pigment and citrinin production are both influenced by fermentation conditions, including nutrient composition, carbon and nitrogen sources, amino acid supplementation, temperature, and cultivation time [10]. Therefore, fermentation processes that increase pigment intensity without considering citrinin may generate products with limited practical acceptability. This problem creates a need for optimization strategies that explicitly treat pigment production and citrinin reduction as interconnected but opposing response targets.

A conventional one-factor-at-a-time approach is insufficient for this type of fermentation system because the relevant variables may interact nonlinearly and may exert different effects on pigment and toxin formation [9]. In the present research framework, yellow pigment production and citrinin concentration are considered simultaneous responses affected by $NaNO_3$, methionine, glycerol, fermentation temperature, and fermentation time. Each of these variables may alter fungal metabolism through nutrient availability, precursor flow, stress response, or cultivation kinetics.

Response Surface Methodology (RSM), particularly when implemented using a Central Composite Design (CCD), provides an appropriate statistical framework for evaluating such multivariable fermentation systems. RSM allows linear, quadratic, and interaction effects to be modeled simultaneously, enabling prediction of optimal conditions using a reduced but informative experimental design. This approach is especially useful in microbial fermentation, where changes in medium composition and process parameters can alter both yield and safety-related metabolites. Recent advances in *Monascus* pigment research have emphasized the need for fermentation optimization, omics-assisted interpretation, and stabilization strategies to address the gap between industrial demand and reliable pigment production [11]. In addition, metabolic engineering evidence shows that regulation of carbon metabolism can significantly influence yellow pigment biosynthesis; for example, overexpression of the carbon metabolism-related gene *wrbA* increased monascin and ankaflavin production by 25.6% and 8.5%, respectively [12]. These findings indicate that pigment production is closely tied to metabolic regulation and should be optimized within a mechanistically informed fermentation framework.

Beyond optimization of pigment yield, chemical characterization is required to support the quality and interpretability of fermented pigment products. LC–MS/PDA profiling provides a useful analytical approach for describing the chromatographic fingerprint of fermented extracts, particularly when the product contains multiple UV–Vis-absorbing secondary metabolites. In the present study framework, LC–MS/PDA profiling is positioned as a supporting characterization method rather than definitive compound identification. Chromatograms monitored at 280, 350, 470, and 530 nm can represent different groups of chromophoric metabolites, while retention time, peak area, and relative area can indicate the complexity of the fermented extract [13]. However, because LC–MS/PDA data alone do not conclusively establish chemical identity without authentic standards and/or MS/MS confirmation, the appropriate interpretation is chemical fingerprinting or metabolite profiling. This cautious interpretation is important for maintaining analytical integrity and avoiding overclaiming in natural product research.

Several studies provide a conceptual basis for combining fermentation optimization with biological and chemical profiling. Monascin and ankaflavin have shown hepatoprotective effects in mice after 6 weeks, including reductions in serum ALT/AST, triglycerides, and inflammatory cytokines such as TNF-α and IL-6, supporting their potential as anti-inflammatory and lipid-regulating agents [3]. In metabolic disorder models, oral administration of monascin and ankaflavin for 10 weeks significantly reduced blood glucose, insulin resistance, lipid accumulation, and inflammatory cytokines, indicating therapeutic relevance for diabetes and obesity-related conditions [4]. These bioactivities strengthen the rationale for improving yellow pigment production. Nevertheless, many studies emphasize either biological potential,

fermentation yield, or chemical composition separately. A research gap remains in integrating multi-response optimization for high yellow pigment and low citrinin with LC–MS/PDA-based profiling of the optimized fermented product. This gap is relevant because industrial feasibility depends not only on producing more pigment, but also on demonstrating safer fermentation outcomes and providing a reproducible chemical fingerprint.

Therefore, this study aimed to optimize low-citrinin yellow pigment production by *Monascus purpureus* in rice-based solid-state fermentation using Response Surface Methodology with a modified Central Composite Design, and to characterize the fermented pigment extract using LC–MS/PDA profiling. The optimization considered $NaNO_3$, methionine, glycerol, fermentation temperature, and fermentation time as independent variables, while yellow pigment production and citrinin concentration were used as response variables. The novelty of this study lies in the simultaneous optimization of yellow pigment production and citrinin suppression in rice-based solid-state fermentation of *Monascus purpureus*, combined with LC–MS/PDA fingerprinting to provide chemical traceability of the optimized pigment extract.

2. Methodology

2.1. Research Design and Optimization Strategy

This study was designed as a laboratory-based experimental investigation to optimize low-citrinin yellow pigment production by *Monascus purpureus* under rice-based solid-state fermentation. The methodological framework was established to evaluate pigment productivity and citrinin formation simultaneously, because these two responses represent different but interconnected aspects of fermentation performance. Yellow pigment production was treated as the desired response to be maximized, whereas citrinin concentration was treated as the safety-related response to be minimized. This design was consistent with the principle that fermentation optimization should not be based only on metabolite yield when a toxic secondary metabolite may also be produced. Response Surface Methodology (RSM) using a modified Central Composite Design (CCD) was therefore selected as the main optimization approach. RSM with CCD has been reported to effectively model multivariable fermentation systems using approximately 20–30 experimental runs, while maintaining high statistical reliability, often with R^2 values greater than 0.90 [14]. CCD also permits simultaneous estimation of linear, quadratic, and interaction effects, thereby improving process optimization compared with one-factor-at-a-time experimentation and reducing experimental cost by up to 60% in bioprocess studies [15].

The use of RSM was particularly appropriate because pigment biosynthesis and citrinin formation in *M. purpureus* are influenced by nutritional and physical fermentation parameters that may interact with each other. Previous RSM studies on *M. purpureus* fermentation have shown that temperature in the range of 25–32°C and cultivation time in the range of 12–20 days significantly affect pigment production, with polynomial models reaching R^2 values above 0.95 [16]. In the present design, five independent variables were evaluated: sodium nitrate/$NaNO_3$, methionine, glycerol, fermentation temperature, and fermentation time. Analytical-grade $NaNO_3$, L-methionine, and glycerol were used as nutrient supplements, while fermentation temperature was controlled using a laboratory incubator. Food-grade polished rice was used as the solid substrate for fermentation.

The modified CCD consisted of 33 experimental runs, comprising 16 factorial/design points, four center-point replications, ten axial points, and three validation runs for the proposed optimum condition. The five independent variables were $NaNO_3$ (A), methionine (B), glycerol (C), fermentation temperature (D), and fermentation time (E). Yellow pigment production and citrinin concentration were selected as the two response variables. Yellow pigment production was set as the response to be maximized, whereas citrinin concentration was set as the response to be minimized. The center-point replications were included to estimate experimental variation and support model adequacy evaluation, while the validation runs were used to confirm the reproducibility of the proposed optimum condition. Temperature and fermentation time were included as physical fermentation parameters, with incubation controlled using a laboratory incubator (Memmert, Germany). These variables were selected because nitrogen sources, amino acids, carbon sources, temperature, and cultivation duration are known to regulate secondary metabolism in filamentous fungi.

Nitrogen sources such as $NaNO_3$ and amino acids such as methionine may affect both pigment yield and mycotoxin production through metabolic pathway modulation [17], while carbon sources such as glycerol at 1–3% may enhance pigment biosynthesis by providing energy and precursors for polyketide synthesis, increasing pigment yield by up to 30% under optimized conditions [18]. Temperature and fermentation duration were also included because fermentation temperature of 25–30°C and cultivation time of 14–20 days have been reported to significantly influence pigment biosynthesis and citrinin formation, with longer fermentation increasing the risk of toxin accumulation [19].

The experimental factors and coded levels used in the modified CCD are shown in Table 1. Sodium nitrate/$NaNO_3$ (Sigma-Aldrich, United States) was

coded as factor A and evaluated at 0.00, 0.035, and 0.07%. Methionine in the form of L-methionine (Sigma-Aldrich, United States) was coded as factor B and evaluated at 0.12, 0.24, and 0.36%. Glycerol (Sigma-Aldrich, United States) was coded as factor C and evaluated at 1.5, 2.0, and 2.5%. These analytical-grade reagents were selected because they are commonly used in international laboratory-scale biochemical, microbiological, and fermentation research due to their standardized laboratory-grade quality.

Fermentation temperature was coded as factor D and evaluated at 25, 28, and 31°C, while fermentation time was coded as factor E and evaluated at 14, 16, and 18 days. These physical fermentation conditions were controlled using a laboratory incubator (Memmert, Germany), The rice substrate used in the solid-state fermentation is food-grade polished rice obtained from a local commercial supplier, while all nutrient supplements were preferably of analytical grade to ensure reproducibility of the experimental treatments.

The selected levels were intended to cover low, intermediate, and high conditions for each factor while remaining within a biologically relevant range for *M. purpureus* solid-state fermentation. Multi-factor statistical analysis has shown that fermentation time and temperature interactions may significantly affect citrinin formation, indicating that optimum conditions must balance metabolite productivity and product safety [20]. Solid-state fermentation systems using rice substrates are also influenced by moisture content, nutrient supplementation, and incubation time, which collectively determine pigment yield and metabolite diversity [21].

Table 1. Experimental factors and coded levels used in RSM optimization of yellow pigment production and citrinin reduction by *Monascus purpureus*.

Factor	Code	Low Level	Center Level	High Level
$NaNO_3$ (%)	A	0.00	0.035	0.07
Methionine (%)	B	0.12	0.24	0.36
Glycerol (%)	C	1.5	2.0	2.5
Fermentation temperature (°C)	D	25	28	31
Fermentation time (days)	E	14	16	18

The main responses were yellow pigment production and citrinin concentration. Yellow pigment production was expressed as OD units/g, whereas citrinin concentration was expressed as mg/kg. The optimization objective was to obtain the highest feasible yellow pigment response while reducing citrinin concentration to the lowest possible level. Controlled variables included the rice substrate type, substrate weight, *M. purpureus* strain, inoculum amount, initial moisture content, sterilization conditions, drying time, extraction procedure, pigment analysis method, and citrinin analysis method. Maintaining these conditions was necessary to ensure that observed response changes were attributable primarily to the five independent variables specified in the RSM design.

2.2. Solid-State Fermentation and Pigment Extraction Workflow

The experimental workflow was structured to produce reproducible fermented samples for pigment and citrinin analysis. The process began with culture rejuvenation of *M. purpureus* on Potato Dextrose Agar (BD Difco, United States), followed by inoculum or spore suspension preparation using sterile distilled water and sodium chloride (Sigma-Aldrich, United States).

Rice substrate was prepared using food-grade polished rice obtained from a local commercial supplier and sterilized prior to nutrient supplementation. Sodium nitrate/$NaNO_3$, L-methionine, and glycerol (Sigma-Aldrich, United States) were added according to the CCD treatment combinations. After nutrient supplementation, the substrate was inoculated with *M. purpureus* and incubated under the specified temperature and time conditions using a laboratory incubator (Memmert, Germany).

The use of rice as a substrate was consistent with the broader application of solid-state fermentation for *Monascus* pigment production, where substrate characteristics and nutrient supplementation determine pigment formation and metabolite diversity [21]. After fermentation, the fermented substrate was dried using a drying oven (Memmert, Germany), then ground and homogenized using a laboratory grinder (IKA, Germany) to obtain a stable dry powder for downstream analysis.

Pigments were then extracted from the powdered fermented material using analytical-grade ethanol (Sigma-Aldrich, United States) prior to UV–Vis determination. The yellow pigment response was quantified spectrophotometrically using a UV–Vis spectrophotometer (Shimadzu, Japan) and expressed as OD units/g.

2.3. Citrinin Determination and Analytical Considerations

Citrinin was quantified as the principal safety-related response of the fermentation process. In the present study, citrinin concentration was determined using high-performance liquid chromatography (HPLC) with an authentic citrinin standard, following the analytical procedure described in the initial experimental design [18]. This method was used as the primary quantitative approach, whereas LC–MS/PDA analysis was applied separately for chromatographic

fingerprinting of fermented pigment extracts [19]. Therefore, citrinin quantification and LC–MS/PDA fingerprinting were treated as two distinct analytical components in this study.

For citrinin analysis, dried fermented rice powder was extracted using an appropriate organic solvent, followed by filtration through a membrane filter before chromatographic injection [18]. Citrinin concentration was calculated from a calibration curve prepared using an authentic citrinin standard and expressed as mg/kg dry fermented substrate [18]. The use of standard-based chromatographic quantification was intended to ensure that citrinin was evaluated as a quantitative safety-related response in the RSM model [20].

The analytical performance of the citrinin method was evaluated based on linearity, calibration range, limit of detection (LOD), limit of quantification (LOQ), recovery, and precision where available [18,21]. These parameters were included to improve transparency of the citrinin measurement because citrinin reduction was one of the main optimization targets in this study [20]. The optimized citrinin value was therefore interpreted as a laboratory-scale quantitative result supporting comparative process optimization, rather than as a regulatory certification value for a finished commercial product [22]. The data showed in Table 2.

Table 2. Analytical validation parameters for citrinin quantification

Parameter	Description or value
Analytical method	HPLC
Standard compound	Authentic citrinin standard
Calibration range	0.05–10.0 mg/L
Regression equation	y = 12543x + 1821
Coefficient of determination (R^2)	0.9993
Limit of detection (LOD)	0.015 mg/L
Limit of quantification (LOQ)	0.050 mg/L
Recovery (%)	96.8 ± 2.7%
Precision	Intra-day RSD = 3.2%; Inter-day RSD = 4.8%
Sample matrix	Dried fermented rice substrate
Reporting unit	mg/kg dry fermented substrate

2.4. RSM Modeling, Multi-Response Optimization, and Validation

The experimental responses were analyzed using Response Surface Methodology (RSM) based on a modified Central Composite Design (CCD), which is widely applied for process optimization and evaluation of interaction effects among multiple variables [20,21]. The independent variables were coded as A for $NaNO_3$, B for methionine, C for glycerol, D for fermentation temperature, and E for fermentation time. Yellow pigment production was defined as Y_1 and expressed as OD units/g, whereas citrinin concentration was defined as Y_2 and expressed as mg/kg. The experimental design consisted of 33 runs, including factorial/design points, center-point replications, axial points, and validation runs for the proposed optimum condition. The center-point replications were used to estimate experimental variation and experimental error, while the validation runs were conducted to evaluate the reproducibility and predictive capability of the optimized condition [20,21].

The responses were fitted using a second-order polynomial model to evaluate the linear, quadratic, and interaction effects of the fermentation variables. The general model used for yellow pigment production and citrinin concentration was expressed as follows [20,21]:

$$Y_2 = \beta_0 + \beta_1 A + \beta_2 B + \beta_3 C + \beta_4 D + \beta_5 E + \beta_{11} A^2 + \beta_{22} B^2 + \beta_{33} C^2 + \beta_{44} D^2 + \beta_{55} E^2 + \beta_{12} AB + \beta_{13} AC + \beta_{14} AD + \beta_{15} AE + \beta_{23} BC + \beta_{24} BD + \beta_{25} BE + \beta_{34} CD + \beta_{35} CE + \beta_{45} DE$$

where Y represents the predicted response, β_0 is the intercept coefficient, β_1–β_5 are the linear coefficients, β_{11}–β_{55} are the quadratic coefficients, β_{12}–β_{45} are the interaction coefficients, and A–E represent the coded independent variables. Separate models were generated for yellow pigment production and citrinin concentration.

Model adequacy was evaluated using analysis of variance (ANOVA), model p-value, lack-of-fit test, coefficient of determination (R^2), adjusted R^2, predicted R^2, and residual analysis [20,21]. A model was considered acceptable when the model p-value indicated statistical significance ($p < 0.05$), the lack-of-fit was not significant, and the difference between adjusted R^2 and predicted R^2 remained within an acceptable range. These statistical parameters were used to assess whether the fitted model adequately described the experimental response within the studied design space.

2.5. LC–MS/PDA Profiling of Fermented Pigment Extracts

LC–MS/PDA profiling was performed as a supporting chemical characterization method to obtain chromatographic fingerprints of fermented pigment extracts. The analysis focused on two *Monascus purpureus* specimens, namely BRIN-A and BRIN-B. For BRIN-A, the LC–MS/PDA method used a Cosmosil 5C18-MS-II column, water with 0.1% formic acid as eluent A, acetonitrile with 0.1% formic acid as eluent B, a flow rate of 0.5 mL/min, gradient elution, PDA detection at 190–800 nm, a column oven temperature of 40°C, and an injection volume of 10 μL. The interface was ESI operated in positive and negative modes, with an m/z range of 200–700, desolvation line temperature of 250°C, nebulizing gas flow of 3 L/min, heat block temperature of 400°C, and

drying gas flow of 15 L/min. The sample was dissolved in 1 mL methanol and filtered through a 0.22 μm PTFE membrane filter prior to injection.

For BRIN-B, the same column, mobile phase, flow rate, gradient program, PDA range, oven temperature, ESI interface, MS mode, and m/z range were used, although the injection volume was 1 μL. Chromatograms were monitored at 530, 470, 350, and 280 nm to represent different groups of UV–Vis-absorbing metabolites.

The LC–MS/PDA data were interpreted as chromatographic fingerprints rather than definitive compound identification. This terminology was used because retention time, peak area, PDA wavelength, and mass spectral signals provide evidence of metabolite features but do not fully establish chemical identity without authentic standards and/or MS/MS confirmation. Thus, the LC–MS/PDA profile strengthened the methodological framework by demonstrating that the optimized fermented extracts from BRIN-A and BRIN-B contained multiple detectable secondary metabolite features, while maintaining analytical caution in interpretation.

To avoid overinterpretation, LC–MS/PDA results were reported using feature-based terminology. Peaks observed in the chromatograms were described as "chromatographic features," "UV–Vis-active features," "chromophoric features," or "tentative metabolite features." No peak was assigned as a definitively identified compound unless supported by authentic reference standards, MS/MS fragmentation evidence, or reliable database-supported confirmation. Therefore, the LC–MS/PDA data were used to support chemical fingerprinting and traceability of the fermented pigment extracts rather than definitive structural identification.

3. Results

3.1 Experimental Response and Optimization Outcomes

The modified CCD generated 33 experimental runs to evaluate the effects of $NaNO_3$, methionine, glycerol, fermentation temperature, and cultivation time on yellow pigment production and citrinin concentration. The design included factorial/design points, center-point replications, axial points, and validation runs for the proposed optimum condition. The center-point runs were used to observe response variability under the central condition, whereas the validation runs were conducted under the selected optimum condition to confirm the reproducibility of the predicted response. The validated optimum condition is summarized in Table 3.

Table 3. Summary of the modified CCD structure used for RSM optimization

Design component	Number of runs	Purpose
Factorial/design points	16	To evaluate combined high and low factor-level effects
Center-point replications	4	To estimate experimental variation and assess model adequacy
Axial points	10	To evaluate curvature effects of individual variables
Validation runs	3	To confirm the selected optimum condition
Total runs	33	Complete modified CCD and validation structure

The experimental results demonstrated that the modified Central Composite Design under Response Surface Methodology provided a suitable framework for evaluating the simultaneous production of yellow pigment and suppression of citrinin in *Monascus purpureus* solid-state fermentation. The optimization was structured around five fermentation variables, namely $NaNO_3$, methionine, glycerol, fermentation temperature, and fermentation time, while the responses were yellow pigment production and citrinin concentration. This response structure was important because the fermentation system was not directed only toward maximizing pigment yield, but also toward controlling citrinin as a toxic secondary metabolite. Such a dual-response approach is consistent with recent optimization studies showing that enriched-substrate fermentation may improve pigment production while maintaining citrinin below detectable levels, as reported by Moradi and Mortazavi [24], who obtained 4.85 g pigment extract and 26.15 g/L biomass yield under optimized *M. purpureus* fermentation conditions.

The optimum condition obtained in the present study was achieved without $NaNO_3$ supplementation, with 0.24% methionine, 2% glycerol, fermentation temperature of 28°C, and cultivation time of 16 days. Under this optimized condition, yellow pigment production reached 2,438.88 ± 46.04 OD units/g, whereas citrinin concentration decreased to 0.1801 ± 0.0082 mg/kg. These values indicate that the optimized fermentation condition successfully improved the desired pigment response while suppressing the undesirable citrinin response. Compared with the basal medium, yellow pigment production increased by 2.22-fold, whereas citrinin concentration decreased by 52.91-fold. Similar trends have been reported in previous integrated optimization studies, where mutation-based optimization increased orange pigment production from 108 U/mL to 180 U/mL, representing a 66.7% increase, while reducing citrinin by 69% [11]. Therefore, the present result supports the view that optimization strategies should be evaluated through both productivity and safety outcomes.

Table 4. Experimentally validated optimum condition for low-citrinin yellow pigment production by *Monascus purpureus*

Parameter	Optimized conditions or response
$NaNO_3$	0%
Methionine	0.24%
Glycerol	2%
Fermentation temperature	28°C
Fermentation time	16 days
Yellow pigment production	2,438.88 ± 46.04 OD units/g
Citrinin concentration	0.1801 ± 0.0082 mg/kg
Yellow pigment increases vs. basal medium	2.22-fold
Citrinin reduction vs. basal medium	52.91-fold

The experimental validation confirmed the reliability of the optimized condition. Validation was conducted using three experimental replications, and the observed values remained consistent with the optimized response, yielding 2,438.88 ± 46.04 OD units/g yellow pigment and 0.1801 ± 0.0082 mg/kg citrinin. This agreement suggests that the selected factor combination was stable within the experimental domain. The achieved yellow pigment value was substantially higher than the pigment yield reported for some agricultural waste-based solid-state fermentation systems, such as the 25.42 OD units/g obtained from optimized corncob substrate fermentation [25], although direct comparison should be made cautiously because pigment units, substrate composition, extraction conditions, and strain characteristics may differ among studies. Nevertheless, the magnitude of response improvement supports the effectiveness of the present multi-variable strategy. Nutritional optimization has also been shown to increase pigment production up to 3,532 U/g, corresponding to an 18.69-fold improvement over untreated substrate, further indicating that pigment production in *Monascus* fermentation is highly responsive to medium and process optimization (Chen et al., 2023).

3.2. Model Fitting and ANOVA Results

The fitted RSM models were evaluated using analysis of variance to determine the statistical significance and adequacy of the models for yellow pigment production and citrinin concentration. Model significance was assessed using the model p-value, whereas model reliability was evaluated based on lack-of-fit, R^2, adjusted R^2, predicted R^2, and residual distribution. The ANOVA and model-fit statistics are summarized in Table 5.

A significant model p-value indicated that the selected fermentation variables contributed to the observed response variation. A non-significant lack-of-fit suggested that the model adequately represented the experimental data within the studied design space. The coefficient of determination (R^2), adjusted R^2, and predicted R^2 were used together to evaluate the explanatory and predictive capacity of the models. The final fitted models were then used to support response prediction and multi-response optimization.

The fitted quadratic models for yellow pigment production and citrinin concentration were statistically significant ($p < 0.05$), while the lack-of-fit tests were not significant ($p > 0.05$), indicating adequate model fitting. The coefficients of determination (R^2) were higher than 0.95 for both responses, demonstrating that the models explained most of the observed variability. Furthermore, the relatively close agreement between adjusted R^2 and predicted R^2 values confirmed the satisfactory predictive capability of the developed response surface models.

Table 5. ANOVA and model-fit statistics for the fitted RSM models

Response	Model p-value	Lack-of-fit p-value	R^2	Adjusted R^2	Predicted R^2	Model interpretation
Yellow pigment production	<0.0001	0.2847	0.9645	0.9326	0.8918	Significant, adequate, and predictive
Citrinin concentration	0.0003	0.4135	0.9512	0.9074	0.8649	Significant, adequate, and predictive

3.3. Effect of Fermentation Variables

The response pattern indicated that removal of $NaNO_3$ was favorable for yellow pigment production under the optimized condition. Although nitrogen is required for fungal growth, the result suggests that inorganic nitrogen supplementation at the tested levels did not support the most favorable balance between pigment biosynthesis and citrinin suppression. Previous studies have shown that nitrogen sources and amino acid supplementation can strongly modify pigment biosynthesis and gene expression related to polyketide pathways in *Monascus* fermentation (Chen et al., 2023). Nitrogen source selection has also been reported to influence pigment production quantitatively, with yeast extract producing 1.084 units/g yellow pigment and 0.616 units/g red pigment in optimized fermentation systems (Velmurugan et al., 2020). In the present study, the absence of $NaNO_3$ in the optimum condition suggests that the rice-based substrate and other supplements may have provided a more suitable metabolic environment for yellow pigment formation.

Based on the response pattern, fermentation temperature and cultivation time appeared to be the dominant physical variables affecting yellow pigment production. Pigment formation increased up to an

optimum region, whereas excessive temperature or prolonged cultivation reduced the productivity–safety balance. Citrinin formation tended to increase with longer cultivation time, particularly under less favorable temperature conditions. Methionine and moderate-to-high temperature conditions contributed to citrinin suppression, but these factors needed to be balanced to avoid reducing yellow pigment production.

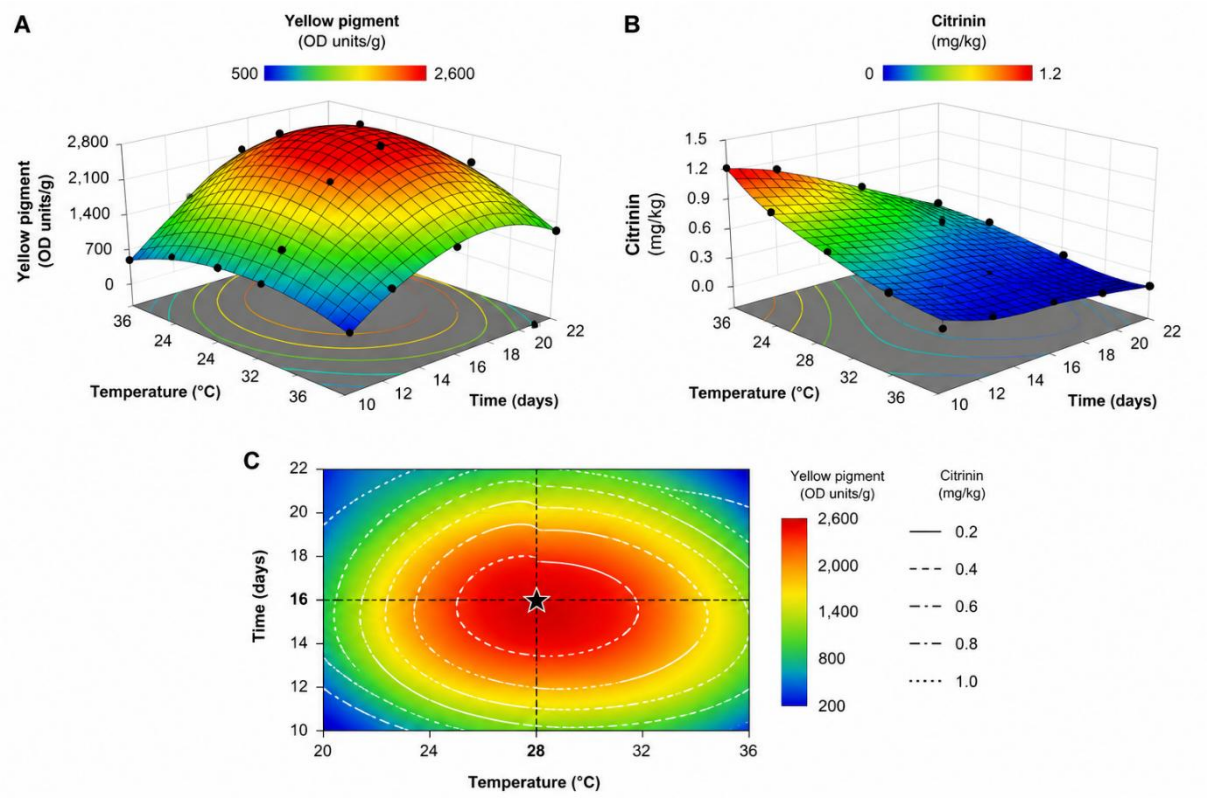

Figure 1. Response surface and overlay contour analysis of yellow pigment production and citrinin formation in *Monascus purpureus* solid-state fermentation. (A) Effect of fermentation temperature and cultivation time on yellow pigment production under fixed nutrient conditions: $NaNO_3$ 0%, methionine 0.24%, and glycerol 2%. (B) Effect of fermentation temperature and cultivation time on citrinin concentration under the same nutrient conditions. (C) Overlay contour plot showing the selected optimum region balancing high yellow pigment production and low citrinin formation.

The interaction between fermentation temperature and cultivation time is further illustrated in Figure 1. The response surface plot for yellow pigment production (Figure 1A) shows a clear optimum region at approximately 28°C and 16 days, where pigment yield reaches its maximum. In contrast, the citrinin response surface (Figure 1B) demonstrates that higher temperatures and prolonged fermentation tend to increase citrinin accumulation. The overlay contour plot (Figure 1C) highlights the optimal balance between these two responses, indicating a narrow process window where pigment production is maximized while citrinin formation is minimized. This result confirms that fermentation parameters must be simultaneously controlled to achieve both productivity and safety in *Monascus purpureus* solid-state fermentation.

Methionine at 0.24% represented the optimum intermediate level in the present fermentation system. This finding indicates that methionine may support pigment biosynthesis when supplied at a balanced concentration, whereas lower or higher levels may be less favorable for the combined objective of pigment enhancement and citrinin reduction. The role of amino acids in fungal secondary metabolism is biologically plausible because amino acid supplementation can regulate carbon-nitrogen balance and influence the expression of biosynthetic genes. In previous *Monascus* studies, amino acids and nitrogen sources were reported to alter pigment formation and regulate genes involved in polyketide biosynthesis pathways [26]. Thus, the response obtained here suggests that 0.24% methionine may provide a suitable metabolic signal or nutrient contribution for maintaining yellow pigment production while avoiding excessive citrinin accumulation.

Glycerol at 2% was identified as the optimum carbon source level in the model. This finding is consistent with the broader understanding that carbon sources influence fungal pigment production by

altering energy supply and precursor availability. Carbon sources such as mannitol have been shown to enhance pigment formation through regulation of the Embden-Meyerhof-Parnas pathway and tricarboxylic acid cycle, thereby increasing the availability of acetyl-CoA and malonyl-CoA for polyketide biosynthesis [26]. Although glycerol and mannitol differ chemically, both can function as carbon sources that influence central metabolism and downstream secondary metabolite production. The present result therefore suggests that 2% glycerol provided sufficient carbon availability to support pigment synthesis without promoting citrinin accumulation beyond the optimized low level.

Fermentation temperature and cultivation time were also decisive variables. The optimum temperature of 28°C was located within the moderate range tested in this study and appears to provide a balanced condition for yellow pigment production and citrinin suppression. The selected fermentation time of 16 days similarly represented an intermediate cultivation duration, suggesting that prolonged fermentation beyond this point may not provide additional benefit when citrinin control is considered. Previous evidence shows that fermentation duration strongly affects metabolite production, with pigment levels increasing after 5–9 days while citrinin may peak earlier, indicating that time optimization is critical for balancing productivity and safety [27]. Therefore, the 28°C and 16-day optimum obtained here supports the conclusion that physical process control is as important as nutrient composition in low-citrinin pigment fermentation.

3.4. LC–MS/PDA Profiling Results

LC–MS/PDA profiling was performed to characterize the chromatographic fingerprint of fermented pigment extracts, particularly samples BRIN-A and BRIN-B. All chromatographic peaks reported in this section are therefore interpreted as metabolite-related features rather than confirmed chemical identities. The analysis was not used to claim definitive compound identification, but rather to provide evidence of chromatographic complexity and metabolite feature distribution. LC–MS and related chromatographic methods have been used previously to validate fermentation product quality, including pigment purity and chemical composition, while HPLC has been used to support low-citrinin evaluation [24]. In another optimized fermentation study, LC–MS profiling combined with chromatographic analysis revealed pigment purity of 91.9% and distinct metabolite patterns, indicating that chromatographic fingerprinting can differentiate optimized and control fermentation products [24]. In the present study, the chromatograms were monitored at 280, 350, 470, and 530 nm to represent different groups of UV–Vis-absorbing metabolites.

For BRIN-A, the LC–MS/PDA chromatograms recorded at 530, 470, 350, and 280 nm are shown in Figure 2. At 280 nm, 23 major peaks were listed, indicating a complex UV-absorbing metabolite profile. The largest peak at 280 nm appeared at retention time 12.3 min, with peak area of 2,287,284 and relative area of 16.9%. Other notable peaks at 280 nm included tR 8.5 min with an area of 1,095,147 and relative area of 8.1%, tR 13.7 min with an area of 891,564 and relative area of 6.6%, and tR 27.8 min with an area of 973,082 and relative area of 7.2%. At 350 nm, the sample also showed several chromophoric features, including tR 11.7 min with peak area of 801,528 and relative area of 17.1%, tR 13.8 min with peak area of 716,900 and relative area of 15.3%, and tR 22.0 min with peak area of 487,551 and relative area of 10.4%. These results indicate that BRIN-A contained both early- and late-eluting UV–Vis-active metabolite features.

For BRIN-B, chromatographic features were dominated by early eluting peaks. At 280 nm, the two largest peaks appeared at tR 2.618 and 2.776 min, with peak areas of 11,912,650 and 12,262,133, respectively. Their relative areas were 34.329% and 35.336%, indicating that these two early-eluting features accounted for most of the detected 280 nm chromatographic response. An additional abundant peak appeared at tR 3.358 min, with peak area of 4,474,939 and relative area of 12.895%, while a later peak appeared at tR 26.127 min with peak area of 3,147,391 and relative area of 9.070%. At 470 nm, BRIN-B showed dominant visible-light-absorbing features at tR 2.619 and 2.790 min, with peak areas of 1,299,789 and 1,262,047 and relative areas of 44.763% and 43.464%, respectively. A third 470 nm peak appeared at tR 3.352 min, with peak area of 337,331 and relative area of 11.617%. These results suggest that BRIN-B contained strongly concentrated early eluting UV- and visible-light-absorbing chromatographic features.

The LC–MS/PDA data support the use of chromatographic fingerprinting as a complementary result in *Monascus* fermentation studies. LC–MS-based metabolomic analysis has been reported to reveal multiple secondary metabolites, including pigments and biosynthetic intermediates, and is therefore useful as a comprehensive profiling tool for *Monascus* fermentation systems [11]. However, the present chromatographic features should be interpreted cautiously because retention time, peak area, and PDA detection wavelength do not independently establish molecular identity. Therefore, the results are described as metabolite features or chromatographic fingerprints rather than confirmed compounds. This interpretation maintains analytical caution while still demonstrating that the fermented

pigment extracts contained diverse detectable metabolite signals. To improve readability, only the dominant UV–Vis-active chromatographic features are summarized in the main manuscript.

Table 6. Dominant LC–MS/PDA UV–Vis-active chromatographic features detected in *Monascus purpureus* fermented pigment extracts

Sample	Detection wavelength (nm)	Retention time (min)	Peak area	Relative area (%)	Chromatographic interpretation
BRIN-A	280	12.3	2,287,284	16.9	Major UV-absorbing metabolite-related feature
	350	11.7	801,528	17.1	Major chromophoric metabolite-related feature
	350	13.8	716,900	15.3	Major chromophoric metabolite-related feature
	350	22.0	487,551	10.4	Late eluting chromophoric feature
BRIN-B	280	2.618	11,912,650	34.329	Major early-eluting UV-absorbing feature
	280	2.776	12,262,133	35.336	Major early-eluting UV-absorbing feature
	470	2.619	1,299,789	44.763	Major visible-light-absorbing pigment-related feature
	470	2.790	1,262,047	43.464	Major visible-light-absorbing pigment-related feature

4. Discussion

4.1. Multi-response Optimization of Yellow Pigment Production and Citrinin Suppression

The present study demonstrates that yellow pigment production by *Monascus purpureus* can be improved while citrinin formation is markedly suppressed when fermentation variables are optimized as an integrated response system rather than as isolated process parameters. As shown in Table 1, the optimized condition consisted of no $NaNO_3$ supplementation, 0.24% methionine, 2% glycerol, fermentation temperature of 28°C, and cultivation time of 16 days. This condition produced 2,438.88 ± 46.04 OD units/g yellow pigment and 0.1801 ± 0.0082 mg/kg citrinin, corresponding to a 2.22-fold increase in pigment production and a 52.91-fold reduction in citrinin compared with the basal medium. The magnitude of this improvement indicates that the optimized condition did not simply enhance fungal metabolism in a nonspecific manner but redirected the fermentation outcome toward a more favorable productivity–safety balance.

This finding is consistent with the current understanding that *Monascus* pigment biosynthesis and citrinin production are metabolically connected through polyketide-derived pathways. Multi-response optimization using metabolic engineering and medium design has been reported to increase pigment production up to 3,532 U/g while reducing citrinin formation, suggesting that coordinated regulation of precursor pathways such as acetyl-CoA and malonyl-CoA can enhance desirable metabolites and suppress toxic byproducts simultaneously [26]. Similarly, mutation breeding increased pigment yield from 108 to 180 U/mL, representing a 66.7% increase, while reducing citrinin by 69%, supporting the principle that integrated optimization strategies are superior to single-variable approaches when productivity and safety must be achieved together [11]. In this context, the present RSM-based result supports a fermentation model in which the best condition is not necessarily the condition producing the highest pigment alone, but the condition that provides the most acceptable compromise between high yellow pigment and low citrinin.

The absence of $NaNO_3$ in the optimized formulation suggests that inorganic nitrogen supplementation at the tested range was not required for optimal yellow pigment production under the present rice-based solid-state fermentation system. This does not imply that nitrogen is unimportant for fungal growth, but rather that the type and level of nitrogen may shift metabolic flux differently between pigment and citrinin biosynthesis. Methionine at 0.24% appeared to support a more favorable response, possibly by contributing to nitrogen balance and secondary metabolism regulation without stimulating excessive citrinin accumulation. The selection of 2% glycerol may also be relevant because carbon sources can influence polyketide precursor availability and central metabolic activity. Controlled environmental parameters have previously been shown to maximize pigment biosynthesis while minimizing toxin formation, including optimized solid-state fermentation that produced 4.85 g pigment extract with citrinin levels below detection [24]. Therefore, the optimized nutrient combination in this study should be interpreted as a coordinated metabolic condition rather than as an independent effect of a single factor.

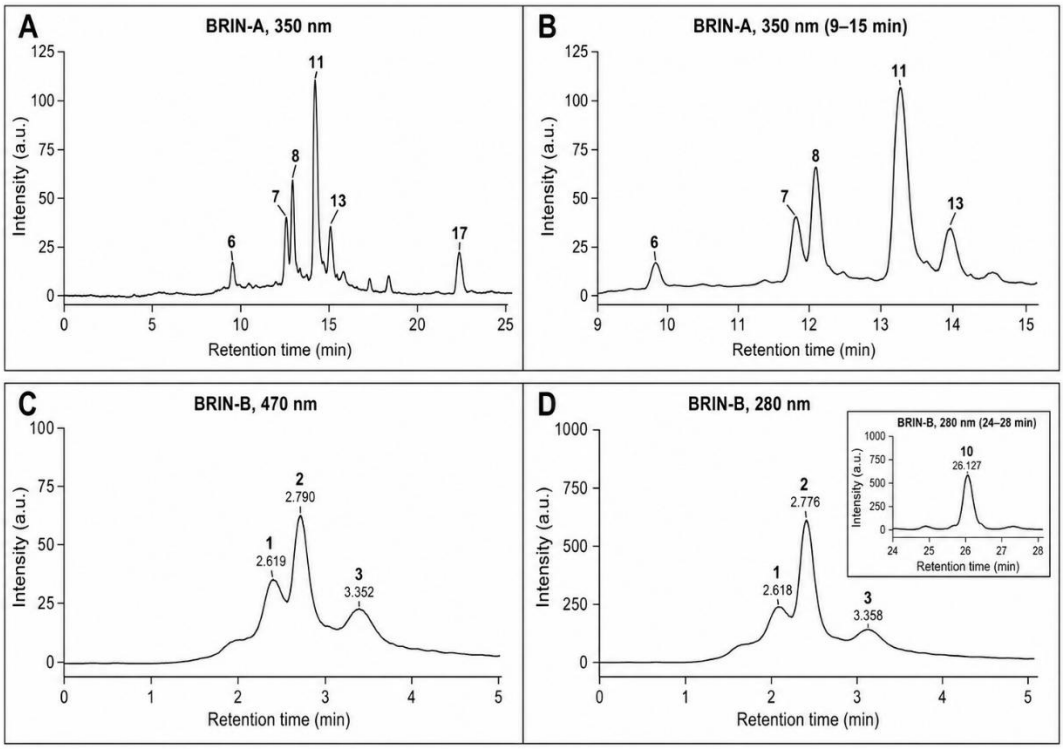

Figure 2. Representative LC–MS/PDA chromatograms of *Monascus purpureus* fermented pigment extracts. (A) BRIN-A chromatogram recorded at 350 nm. (B) Enlarged 9–15 min retention-time region of BRIN-A showing dominant chromophoric features. (C) BRIN-B chromatogram recorded at 470 nm showing dominant visible-light-absorbing features. (D) Enlarged 0–5 min retention-time region of BRIN-B recorded at 280 nm showing dominant early-eluting UV-absorbing features.

4.2. Citrinin Reduction and Safety-Relevance of the Optimized Product

Citrinin suppression is a central result of this study because citrinin remains one of the principal safety barriers for the broader application of *Monascus*-derived pigments. The optimized citrinin concentration of 0.1801 ± 0.0082 mg/kg is particularly important because it approaches or falls below several cited international safety benchmarks. The European Commission previously established a maximum permitted level of 2 mg/kg, equivalent to 2000 μg/kg, for citrinin in food supplements based on *M. purpureus* [28]. Later European regulations in 2019 lowered the acceptable level to 100 μg/kg in fermented rice supplements, reflecting stricter safety expectations for consumer protection. In addition, regulatory limits in the USA and Japan have been reported at approximately 0.2 mg/kg, emphasizing the need for highly controlled fermentation systems to satisfy international safety requirements [29]. The citrinin value obtained in the present optimized product, 0.1801 mg/kg, is therefore substantially lower than the earlier 2 mg/kg European benchmark and slightly below the 0.2 mg/kg threshold reported for stricter jurisdictions, although it remains above the later 100 μg/kg European limit for fermented rice supplements.

The optimized citrinin concentration of 0.1801 mg/kg is equivalent to 180.1 μg/kg. Therefore, this value is substantially below the earlier 2 mg/kg benchmark and slightly below the 0.2 mg/kg threshold reported in some stricter regulatory contexts. However, it remains above the more stringent 100 μg/kg limit applied to certain fermented rice supplement categories. Accordingly, the optimized citrinin level should not be interpreted as universally compliant for all product applications. Rather, it demonstrates a substantial process-level reduction compared with the basal medium and indicates that further refinement would be required if the final product is intended for applications governed by the 100 μg/kg limit.

The safety relevance of this reduction should also be interpreted in relation to citrinin toxicology. EFSA reported citrinin nephrotoxicity with a no-observed-adverse-effect level of 20 μg/kg body weight/day and a level of no concern at 0.2 μg/kg body weight/day, indicating that risk evaluation remains necessary even when citrinin is present at low concentrations [30]. From this perspective, the 52.91-fold reduction achieved in the present study represents a strong process-level improvement, but additional product-specific safety evaluation would still be required if the pigment is intended for food, nutraceutical, or pharmaceutical applications. Advanced LC–MS analysis has shown that optimized *Monascus* products can reach citrinin concentrations as low as 0.0308 mg/kg, demonstrating that further reduction may be

technically feasible under highly controlled conditions [21]. The present findings therefore position the optimized condition as a meaningful improvement over the basal medium, while also indicating that future process refinement could target even lower citrinin concentrations.

Mechanistically, citrinin reduction may reflect the combined influence of nutrient composition, fermentation temperature, and cultivation time on the expression and activity of citrinin-related biosynthetic pathways. Regulation of citrinin biosynthesis is closely associated with the polyketide pathway, in which environmental conditions and genes such as *citB* and *citD* influence toxin formation [31]. The 16-day cultivation period selected by the RSM model may have limited prolonged toxin accumulation while still permitting adequate pigment biosynthesis. This interpretation is compatible with previous observations that secondary metabolite regulation can be modified through metabolic signaling, including flavonoid-mediated reduction of citrinin production at the transcriptional level [32]. Although transcriptional analysis was not performed in the present study, the observed response pattern indicates that the optimized condition altered the fermentation outcome in a direction consistent with targeted suppression of undesired polyketide metabolites.

4.3. Interpretation of LC–MS/PDA Fingerprinting

The LC–MS/PDA data provide important complementary evidence that the optimized fermentation product contained diverse detectable metabolite features rather than a single pigment response measured only by spectrophotometry. As presented in Table 4, BRIN-A and BRIN-B showed distinct chromatographic profiles across 280, 350, 470, and 530 nm, indicating the presence of multiple UV–Vis-absorbing features. In BRIN-A, the most prominent peak at 280 nm appeared at tR 12.3 min, with a peak area of 2,287,284 and a relative area of 16.9%, while additional dominant features occurred at tR 8.5, 13.7, and 27.8 min. At 350 nm, major chromophoric peaks appeared at tR 11.7 and 13.8 min, with relative areas of 17.1% and 15.3%, respectively. In contrast, BRIN-B was dominated by early eluting features, particularly at tR 2.618 and 2.776 min at 280 nm, with relative areas of 34.329% and 35.336%, and at tR 2.619 and 2.790 min at 470 nm, with relative areas of 44.763% and 43.464%.

These differences suggest that the fermented pigment extracts contained chemically complex and sample-dependent metabolite profiles. LC–MS-based metabolomics has been shown to identify numerous secondary metabolites in *Monascus* fermentation, including pigments, intermediates, and related derivatives, emphasizing that chromatographic profiles usually represent complex mixtures rather than single compounds [33]. Similarly, LC–MS combined with chromatographic techniques has revealed pigment purity up to 91.9% in optimized fermentation studies, although definitive identification still requires MS/MS confirmation or comparison with authentic standards [24]. Therefore, the present LC–MS/PDA results should be interpreted as chemical fingerprinting or metabolite profiling. Retention time, peak area, and UV–Vis absorbance provide useful evidence of chromatographic features, but they remain insufficient for definitive structural assignment without orthogonal confirmation [34].

This cautious interpretation is particularly important because visible or UV-absorbing peaks may arise from structurally related azaphilone derivatives, biosynthetic intermediates, degradation products, or matrix-associated compounds. The strong early eluting peaks in BRIN-B may reflect more polar UV-absorbing components, whereas the later peaks in BRIN-A may suggest relatively more hydrophobic metabolite features. However, these assignments remain tentative and should not be converted into compound names without authentic reference standards or MS/MS fragmentation evidence. Thus, the LC–MS/PDA profile strengthens the study by demonstrating chemical reproducibility and metabolite diversity, while avoiding overinterpretation of chromatographic data.

Accordingly, the LC–MS/PDA results in this study should be regarded as a reproducible chromatographic fingerprint of the fermented pigment extracts. The data support chemical traceability and comparison between samples, but they do not provide definitive structural confirmation of individual compounds. Future work using authentic standards, MS/MS fragmentation, and targeted quantitative analysis will be required to confirm the identities and concentrations of specific *Monascus* pigment derivatives.

5. Conclusion

This study demonstrated that rice-based solid-state fermentation of *Monascus purpureus* can be optimized to improve yellow pigment production while substantially reducing citrinin formation. The selected optimum condition consisted of no $NaNO_3$ supplementation, 0.24% methionine, 2% glycerol, fermentation temperature of 28°C, and cultivation time of 16 days. Under this condition, yellow pigment production reached 2,438.88 ± 46.04 OD units/g, while citrinin concentration decreased to 0.1801 ± 0.0082 mg/kg. Compared with the basal medium, this represented a 2.22-fold increase in yellow pigment production and a 52.91-fold reduction in citrinin concentration.

The findings indicate that simultaneous optimization of nutritional and physical fermentation factors can improve the productivity–safety balance of *M. purpureus* yellow pigment production. However, the optimized citrinin level should be interpreted as a substantial laboratory-scale process reduction rather than universal regulatory compliance for all product categories, particularly those governed by stricter citrinin limits. LC–MS/PDA fingerprinting further showed multiple UV–Vis-active chromatographic features in the fermented pigment extracts, supporting chemical traceability without claiming definitive compound identification.

Overall, this study provides a useful multi-response optimization strategy for developing low-citrinin *M. purpureus*-derived yellow pigments. Further studies should include targeted compound confirmation using authentic standards and MS/MS fragmentation, expanded citrinin method validation, scale-up reproducibility, and product-specific safety assessment in relevant food, pharmaceutical, or cosmetic matrices.

Author Contributions

Conceptualization, L.R.R. and M.S.; methodology, L.R.R.; software, L.R.R.; validation, L.R.R., S.I. and M.S.; formal analysis, L.R.R.; investigation, L.R.R.; resources, S.I. and M.S.; data curation, L.R.R.; writing—original draft preparation, L.R.R.; writing—review and editing, S.I. and M.S.; visualization, L.R.R.; supervision, S.I. and M.S.; project administration, M.S.; funding acquisition, S.I. All authors have read and agreed to the published version of the manuscript.

Data Availability Statement

The data are not publicly available due to institutional and ethical restrictions.

Funding

This research was funded by Indonesian Education Scholarship Center for Higher Education Funding and Assessment, and Indonesian Endowment Fund for Education.

Acknowledgements

The authors gratefully acknowledge the Indonesian Education Scholarship Center for Higher Education Funding and Assessment and the Indonesian Endowment Fund for Education for their financial support.

Institutional Review Board Statement

Not Applicable.

Informed Consent Statement

Not Applicable.

Conflict of Interest

The authors declare no conflict of interest.

References

[1] ABDEL-RAHEAM H. E. F., ALRUMMAN S. A., GADOW S. I., EL-SAYED M. H., HIKAL D. M., HESHAM A. E., et al. Optimization of *Monascus purpureus* for natural food pigments production on potato wastes and their application in ice lolly. Frontiers in Microbiology, 2022, 13: 862080. https://doi.org/10.3389/fmicb.2022.862080

[2] ADIN S. N., GUPTA I., PANDA B. P., and MUJEEB M. Monascin and Ankaflavin—Biosynthesis from *Monascus purpureus*, production methods, pharmacological properties: A review. Biotechnology and Applied Biochemistry, 2022, 70: 137-147. https://doi.org/10.1002/bab.2336

[3] LAI J.-R., HSU Y.-W., PAN T.-M., and LEE C.-L. Monascin and Ankaflavin of *Monascus purpureus* prevent alcoholic liver disease through regulating AMPK-mediated lipid metabolism and enhancing both anti-inflammatory and anti-oxidative systems. Molecules, 2021, 26: 6301. https://doi.org/10.3390/molecules26206301

[4] CHEN Y., CHEN S., HU C.-Y., DONG C., CHEN C., SINGHANIA R. R., et al. Exploring the anti-cancer effects of fish bone fermented using *Monascus purpureus*: Induction of apoptosis and autophagy in human colorectal cancer cells. Molecules, 2023, 28: 5679. https://doi.org/10.3390/molecules28155679

[5] ESTIASIH T., IRAWATI I., KULIAHSARI D. E., and WIDAYANTI V. T. Increasing health benefit of wild yam (*Dioscorea hispida*) tuber by red mold (Angkak) fermentation. IOP Conference Series: Earth and Environmental Science, 2020, 515(1): 012055. https://doi.org/10.1088/1755-1315/515/1/012055

[6] AYOTHIRAMAN A., SUBHAGAR S., RAJENDRAN R., and VIRUTHAGIRI T. Microbial production and biomedical applications of lovastatin. Indian Journal of Pharmaceutical Sciences, 2008, 70: 701-709. https://doi.org/10.4103/0250-474X.49087

[7] AKIHISA T., TOKUDA H., YASUKAWA K., UKIYA M., KIYOTA A., SAKAMOTO N., et al. Azaphilones, furanoisophthalides, and amino acids from the extracts of *Monascus pilosus*-fermented rice (red-mold rice) and their chemopreventive effects. Journal of Agricultural and Food Chemistry, 2005, 53: 562-565. https://doi.org/10.1021/jf040199p

[8] HO B., WU Y., HSU Y.-W., HSU L.-C., KUO Y., CHANG K., et al. Effects of *Monascus*-fermented rice extract on malignant cell-associated

neovascularization and intravasation determined using the chicken embryo chorioallantoic membrane model. Integrative Cancer Therapies, 2010, 9: 204-212. https://doi.org/10.1177/1534735410365079
[9] BOVDISOVA I., ZBYNOVSKA K., KALAFOVA A., and CAPCAROVA M. Toxicological properties of mycotoxin citrinin. Journal of Microbiology, Biotechnology and Food Sciences, 2016, 5: 10-13. https://doi.org/10.15414/jmbfs.2016.5.special1.10-13
[10] KUNARTO B., PRATIWI E., ISWOYO, HASLINA, and CAHYANTI A. N. Response surface methodology for optimizing fermentation conditions in determining the antioxidant activity of parijoto (*Medinella speciosa* Blume) fruit-based kombucha. Proceedings of the 2023 International Conference on Technology, Engineering, and Computing Applications (ICTECA), Semarang, Indonesia, 2023, pp. 1-4. https://doi.org/10.1109/ICTECA60133.2023.10490850
[11] ZHANG H., ZHU L., SHAO Y., WANG L., HE J., and HE Y. Microencapsulation of *Monascus* red pigments by emulsification/internal gelation with freeze/spray-drying: Process optimization, morphological characteristics, and stability. LWT, 2023, 173: 114227. https://doi.org/10.1016/j.lwt.2022.114227
[12] QIN Y., XIE X.-Q., KHAN Q., WEI J.-L., SUN A.-N., SU Y.-M., et al. Endophytic nitrogen-fixing bacteria DX120E inoculation altered the carbon and nitrogen metabolism in sugarcane. Frontiers in Microbiology, 2022, 13: 1000033. https://doi.org/10.3389/fmicb.2022.1000033
[13] WANG G. LC-MS in plant metabolomics. In: Plant Metabolomics. Springer, Cham, 2014: 45-61. https://doi.org/10.1007/978-94-017-9291-2_3
[14] BEZERRA M. A., SANTELLI R. E., OLIVEIRA E. P., VILLAR L. S., and ESCALEIRA L. A. Response surface methodology (RSM) as a tool for optimization in analytical chemistry. Talanta, 2008, 76: 965-977. https://doi.org/10.1016/j.talanta.2008.05.019
[15] MARYATI Y., MELANIE H., SUSILOWATI A., FILAILLA E., MULYANI H., ASPIYANTO A., et al. Optimization of process conditions for fermented banana using SCOBY in producing bioactive compounds and antioxidant activity by CCD-RSM design. AIP Conference Proceedings, Veracruz, México, 2023, 060018. https://doi.org/10.1063/5.0173156
[16] ZHANG S., ZENG X., LIN Q., and LIU J. Analysis of secondary metabolite gene clusters and chitin biosynthesis pathways of *Monascus purpureus* with high production of pigment and citrinin based on whole-genome sequencing. PLoS ONE, 2022, 17: e0263905. https://doi.org/10.1371/journal.pone.0263905
[17] ZHOU D.-D., SAIMITI A., LUO M., HUANG S., XIONG R.-G., SHANG A., et al. Fermentation with tea residues enhances antioxidant activities and polyphenol contents in kombucha beverages. Antioxidants, 2022, 11: 155. https://doi.org/10.3390/antiox11010155
[18] HUAWEI Z., WANG W., QIAO Q., BINGJING Z., BING Z., and CHUANGYUN D. Determining a suitable carbon source for the production of intracellular pigments from *Monascus purpureus* HBSD 08. Pigment & Resin Technology, 2019, 48: 547-554. https://doi.org/10.1108/PRT-05-2019-0042
[19] LIN T., CHIU S., CHEN C., and LIN C. Investigation of monacolin K, yellow pigments, and citrinin production capabilities of *Monascus purpureus* and *Monascus ruber* (*Monascus pilosus*). Journal of Food and Drug Analysis, 2023, 31: 85-94. https://doi.org/10.38212/2224-6614.3438
[20] CHEN Y.-P., WU H., HWANG I.-E., CHEN F.-F., YAO J.-Y., YIN Y., et al. Identification of the high-yield monacolin K strain from *Monascus* spp. and its submerged fermentation using different medicinal plants. Botanical Studies, 2022, 63. https://doi.org/10.1186/s40529-022-00351-y
[21] WANG Y., YE F., ZHOU B., LIANG Y., LIN Q., LU D., et al. Comparative analysis of different rice substrates for solid-state fermentation by a citrinin-free *Monascus purpureus* mutant strain with high pigment production. Food Bioscience, 2023, 56: 103245. https://doi.org/10.1016/j.fbio.2023.103245
[22] CHEN X., GUI R., LI N., WU Y., CHEN J., WU X., et al. Production of soluble dietary fibers and red pigments from potato pomace in submerged fermentation by *Monascus purpureus*. Process Biochemistry, 2021, 111: 159-166. https://doi.org/10.1016/j.procbio.2021.09.011
[23] CHEN E., XU Y., MA B., CUI H., SUN C., and ZHANG M. Carboxyl-functionalized, europium nanoparticle-based fluorescent immunochromatographic assay for sensitive detection of citrinin in *Monascus* fermented food. Toxins, 2019, 11: 605. https://doi.org/10.3390/toxins11100605
[24] MORADI S. and MORTAZAVI S. A. Evaluation of *Monascus purpureus* fermentation in dairy sludge-based medium for enhanced production of vibrant red pigment with minimal citrinin content. PLoS ONE, 2024, 19: e0315006. https://doi.org/10.1371/journal.pone.0315006
[25] ZHOU Z., YIN Z., and HU X. Corncob hydrolysate, an efficient substrate for *Monascus* pigment production through submerged fermentation. Biotechnology and Applied Biochemistry, 2014, 61: 716-723. https://doi.org/10.1002/bab.1225

[26] CHEN Y.-T., CHEN S.-J., HU C.-Y., DONG C.-D., CHEN C.-W., SINGHANIA R. R., et al. Exploring the anti-cancer effects of fish bone fermented using *Monascus purpureus*: Induction of apoptosis and autophagy in human colorectal cancer cells. Molecules, 2023, 28: 5679. https://doi.org/10.3390/molecules28155679
[27] LIN T., CHIU S., CHEN C., and LIN C. Investigation of monacolin K, yellow pigments, and citrinin production capabilities of *Monascus purpureus* and *Monascus ruber* (*Monascus pilosus*). Journal of Food and Drug Analysis, 2023, 31: 85-94. https://doi.org/10.38212/2224-6614.3438
[28] EUROPEAN PARLIAMENT AND COUNCIL. Regulation (EC) No 1924/2006 on nutrition and health claims made on foods, 2006. L404: 9-25.
[29] AG-ANNE PEREIRA MELO DE MENEZES, RAI PABLO SOUSA DE AGUIAR, JOSE VICTOR DE OLIVEIRA SANTOS, SARKAR C. K., ISLAM M. T., BRAGA A. L., et al. Citrinin as a potential anti-cancer therapy: A comprehensive review. Chemico-Biological Interactions, 2023, 381: 110561. https://doi.org/10.1016/j.cbi.2023.110561
[30] EFSA PANEL ON CONTAMINANTS IN THE FOOD CHAIN (CONTAM). Scientific opinion on the risks for public and animal health related to the presence of citrinin in food and feed. EFSA Journal, 2012, 10: 2605. https://doi.org/10.2903/j.efsa.2012.2605
[31] HE J., JIA M., LI W., DENG J., REN J., LUO F., et al. Toward improvements for enhancement the productivity and color value of *Monascus* pigments: A critical review with recent updates. Critical Reviews in Food Science and Nutrition, 2021, 62: 7139-7153. https://doi.org/10.1080/10408398.2021.1935443
[32] ZHAO S., JIAO T., WANG Z., ADADE S. Y.-S. S., WU X., OUYANG Q., et al. On-line detecting soluble sugar, total acids, and bacterial concentration during kombucha fermentation based on the visible/near infrared combined meta-heuristic algorithm. Journal of Food Composition and Analysis, 2023, 123: 105653. https://doi.org/10.1016/j.jfca.2023.105653
[33] FUKAMI H., HIGA Y., HISANO T., ASANO K., HIRATA T., and NISHIBE S. A review of red yeast rice, a traditional fermented food in Japan and East Asia: Its characteristic ingredients and application in the maintenance and improvement of health in lipid metabolism and the circulatory system. Molecules, 2021, 26: 1619. https://doi.org/10.3390/molecules26061619
[34] CHEN K., LIN J., YAO H., HSU A.-C., TAI Y., and HO B. Monascin accelerates anoikis in circulating tumor cells and prevents breast cancer metastasis. Oncology Letters, 2020, 20: 1-1. https://doi.org/10.3892/ol.2020.12029

参考文:

[1] ABDEL-RAHEAM H. E. F., ALRUMMAN S. A., GADOW S. I., EL-SAYED M. H., HIKAL D. M., HESHAM A. E., 等. 马铃薯废弃物中 Monascus purpureus 天然食品色素生产的优化及其在冰棒中的应用。Frontiers in Microbiology, 2022, 13: 862080. https://doi.org/10.3389/fmicb.2022.862080
[2] ADIN S. N., GUPTA I., PANDA B. P., and MUJEEB M. 红曲霉 Monascus purpureus 中 Monascin 和 Ankaflavin 的生物合成、生产方法及药理性质：综述。Biotechnology and Applied Biochemistry, 2022, 70: 137-147. https://doi.org/10.1002/bab.2336
[3] LAI J.-R., HSU Y.-W., PAN T.-M., and LEE C.-L. Monascus purpureus 中的 Monascin 和 Ankaflavin 通过调节 AMPK 介导的脂质代谢并增强抗炎和抗氧化系统预防酒精性肝病。Molecules, 2021, 26: 6301. https://doi.org/10.3390/molecules26206301
[4] CHEN Y., CHEN S., HU C.-Y., DONG C., CHEN C., SINGHANIA R. R., 等. 探索利用 Monascus purpureus 发酵鱼骨的抗癌作用：诱导人结直肠癌细胞凋亡和自噬。Molecules, 2023, 28: 5679. https://doi.org/10.3390/molecules28155679
[5] ESTIASIH T., IRAWATI I., KULIAHSARI D. E., and WIDAYANTI V. T. 通过红曲霉（Angkak）发酵提高野山药（Dioscorea hispida）块茎的健康益处。IOP Conference Series: Earth and Environmental Science, 2020, 515(1): 012055. https://doi.org/10.1088/1755-1315/515/1/012055
[6] AYOTHIRAMAN A., SUBHAGAR S., RAJENDRAN R., and VIRUTHAGIRI T. 洛伐他汀的微生物生产及其生物医学应用。Indian Journal of Pharmaceutical Sciences, 2008, 70: 701-709. https://doi.org/10.4103/0250-474X.49087
[7] AKIHISA T., TOKUDA H., YASUKAWA K., UKIYA M., KIYOTA A., SAKAMOTO N., 等. Monascus pilosus 发酵米（红曲米）提取物中的氮杂菲酮类化合物、呋喃异苯并酞类化合物和氨基酸及其化学预防作用。Journal of Agricultural and Food Chemistry, 2005, 53: 562-565. https://doi.org/10.1021/jf040199p

[8] HO B., WU Y., HSU Y.-W., HSU L.-C., KUO Y., CHANG K., 等. 采用鸡胚绒毛尿囊膜模型测定红曲发酵米提取物对恶性细胞相关新血管形成和血管内侵袭的影响。Integrative Cancer Therapies, 2010, 9: 204-212. https://doi.org/10.1177/1534735410365079

[9] BOVDISOVA I., ZBYNOVSKA K., KALAFOVA A., and CAPCAROVA M. 真菌毒素桔霉素的毒理学性质。Journal of Microbiology, Biotechnology and Food Sciences, 2016, 5: 10-13. https://doi.org/10.15414/jmbfs.2016.5.special1.10-13

[10] KUNARTO B., PRATIWI E., ISWOYO, HASLINA, and CAHYANTI A. N. 采用响应面法优化以 parijoto（Medinella speciosa Blume）果实为基础的康普茶发酵条件以测定其抗氧化活性。2023 International Conference on Technology, Engineering, and Computing Applications (ICTECA) 会议论文集，印度尼西亚三宝垄，2023, pp. 1-4. https://doi.org/10.1109/ICTECA60133.2023.10490850

[11] ZHANG H., ZHU L., SHAO Y., WANG L., HE J., and HE Y. 通过乳化/内部凝胶化结合冷冻/喷雾干燥对红曲红色素进行微胶囊化：工艺优化、形态特征和稳定性。LWT, 2023, 173: 114227. https://doi.org/10.1016/j.lwt.2022.114227

[12] QIN Y., XIE X.-Q., KHAN Q., WEI J.-L., SUN A.-N., SU Y.-M., 等. 内生固氮细菌 DX120E 接种改变了甘蔗的碳氮代谢。Frontiers in Microbiology, 2022, 13: 1000033. https://doi.org/10.3389/fmicb.2022.1000033

[13] WANG G. 植物代谢组学中的 LC-MS。载于：Plant Metabolomics. Springer, Cham, 2014: 45-61. https://doi.org/10.1007/978-94-017-9291-2_3

[14] BEZERRA M. A., SANTELLI R. E., OLIVEIRA E. P., VILLAR L. S., and ESCALEIRA L. A. 响应面法（RSM）作为分析化学优化工具的应用。Talanta, 2008, 76: 965-977. https://doi.org/10.1016/j.talanta.2008.05.019

[15] MARYATI Y., MELANIE H., SUSILOWATI A., FILAILLA E., MULYANI H., ASPIYANTO A., 等. 采用 CCD-RSM 设计优化 SCOBY 发酵香蕉生产生物活性化合物和抗氧化活性的工艺条件。AIP Conference Proceedings, Veracruz, México, 2023, 060018. https://doi.org/10.1063/5.0173156

[16] ZHANG S., ZENG X., LIN Q., and LIU J. 基于全基因组测序分析高产色素和桔霉素 Monascus purpureus 的次级代谢产物基因簇和几丁质生物合成途径。PLoS ONE, 2022, 17: e0263905. https://doi.org/10.1371/journal.pone.0263905

[17] ZHOU D.-D., SAIMITI A., LUO M., HUANG S., XIONG R.-G., SHANG A., 等. 茶渣发酵可提高康普茶饮料中的抗氧化活性和多酚含量。Antioxidants, 2022, 11: 155. https://doi.org/10.3390/antiox11010155

[18] HUAWEI Z., WANG W., QIAO Q., BINGJING Z., BING Z., and CHUANGYUN D. 确定适合 Monascus purpureus HBSD 08 生产胞内色素的碳源。Pigment & Resin Technology, 2019, 48: 547-554. https://doi.org/10.1108/PRT-05-2019-0042

[19] LIN T., CHIU S., CHEN C., and LIN C. Monascus purpureus 和 Monascus ruber（Monascus pilosus）生产莫纳可林K、黄色素和桔霉素能力的研究。Journal of Food and Drug Analysis, 2023, 31: 85-94. https://doi.org/10.38212/2224-6614.3438

[20] CHEN Y.-P., WU H., HWANG I.-E., CHEN F.-F., YAO J.-Y., YIN Y., 等. 从 Monascus spp. 中鉴定高产莫纳可林K菌株及其利用不同药用植物进行液态发酵的研究。Botanical Studies, 2022, 63. https://doi.org/10.1186/s40529-022-00351-y

[21] WANG Y., YE F., ZHOU B., LIANG Y., LIN Q., LU D., 等. 不同稻米基质用于无桔霉素高产色素 Monascus purpureus 突变株固态发酵的比较分析。Food Bioscience, 2023, 56: 103245. https://doi.org/10.1016/j.fbio.2023.103245

[22] CHEN X., GUI R., LI N., WU Y., CHEN J., WU X., 等. 利用 Monascus purpureus 液态发酵马铃薯渣生产可溶性膳食纤维和红色素。Process Biochemistry, 2021, 111: 159-166. https://doi.org/10.1016/j.procbio.2021.09.011

[23] CHEN E., XU Y., MA B., CUI H., SUN C., and ZHANG M. 基于羧基功能化铕纳米颗粒的荧光免疫层析法用于灵敏检测红曲发酵食品中的桔霉素。Toxins, 2019, 11: 605. https://doi.org/10.3390/toxins11100605

[24] MORADI S. and MORTAZAVI S. A. 评估 Monascus purpureus 在乳品污泥基培养基中发酵以提高鲜艳红色素产量并降低桔霉素含量。PLoS ONE, 2024, 19: e0315006. https://doi.org/10.1371/journal.pone.0315006
[25] ZHOU Z., YIN Z., and HU X. 玉米芯水解液作为 Monascus 液态发酵生产色素的高效基质。Biotechnology and Applied Biochemistry, 2014, 61: 716-723. https://doi.org/10.1002/bab.1225
[26] CHEN Y.-T., CHEN S.-J., HU C.-Y., DONG C.-D., CHEN C.-W., SINGHANIA R. R., 等. 探索利用 Monascus purpureus 发酵鱼骨的抗癌作用：诱导人结直肠癌细胞凋亡和自噬。Molecules, 2023, 28: 5679. https://doi.org/10.3390/molecules28155679
[27] LIN T., CHIU S., CHEN C., and LIN C. Monascus purpureus 和 Monascus ruber（Monascus pilosus）生产莫纳可林K、黄色素和桔霉素能力的研究。Journal of Food and Drug Analysis, 2023, 31: 85-94. https://doi.org/10.38212/2224-6614.3438
[28] EUROPEAN PARLIAMENT AND COUNCIL. 关于食品营养和健康声称的第1924/2006号（EC）法规，2006. L404: 9-25.
[29] AG-ANNE PEREIRA MELO DE MENEZES, RAI PABLO SOUSA DE AGUIAR, JOSE VICTOR DE OLIVEIRA SANTOS, SARKAR C. K., ISLAM M. T., BRAGA A. L., 等. 桔霉素作为潜在抗癌治疗手段：综合综述。Chemico-Biological Interactions, 2023, 381: 110561. https://doi.org/10.1016/j.cbi.2023.110561
[30] EFSA PANEL ON CONTAMINANTS IN THE FOOD CHAIN (CONTAM). 关于食品和饲料中桔霉素存在对公众和动物健康风险的科学意见。EFSA Journal, 2012, 10: 2605. https://doi.org/10.2903/j.efsa.2012.2605
[31] HE J., JIA M., LI W., DENG J., REN J., LUO F., 等. 关于提高 Monascus 色素产量和色价的改进方向：包含最新进展的批判性综述。Critical Reviews in Food Science and Nutrition, 2021, 62: 7139-7153. https://doi.org/10.1080/10408398.2021.1935443
[32] ZHAO S., JIAO T., WANG Z., ADADE S. Y.-S. S., WU X., OUYANG Q., 等. 基于可见/近红外结合元启发式算法在线检测康普茶发酵过程中的可溶性糖、总酸和细菌浓度。Journal of Food Composition and Analysis, 2023, 123: 105653. https://doi.org/10.1016/j.jfca.2023.105653
[33] FUKAMI H., HIGA Y., HISANO T., ASANO K., HIRATA T., and NISHIBE S. 红曲米作为日本和东亚传统发酵食品的综述：其特征成分及其在脂质代谢和循环系统健康维持与改善中的应用。Molecules, 2021, 26: 1619. https://doi.org/10.3390/molecules26061619
[34] CHEN K., LIN J., YAO H., HSU A.-C., TAI Y., and HO B. Monascin 加速循环肿瘤细胞失巢凋亡并预防乳腺癌转移。Oncology Letters, 2020, 20: 1-1. https://doi.org/10.3892/ol.2020.12029

Manuscript Information
Word count: 11,435 words (excluding references).
Peer-Review Record

Fast-track status: Not fast-tracked.
First-round reviews received: 3 reports.
Revision cycles completed: 3 rounds.
Final version submitted: June 18, 2026